Skeletal Radiol (2012) 41:643–649
DOI 10.1007/s00256-011-1263-7

SCIENTIFIC ARTICLE

Soft-tissue inflammatory myofibroblastic tumors (IMTs) of the limbs: potential and limits of diagnostic imaging

Carlo Masciocchi · Giuseppe Lanni · Laura Conti · Armando Conchiglia · Eva Fascetti · Stefano Flamini · Gino Coletti · Antonio Barile

Received: 21 April 2011 / Revised: 6 July 2011 / Accepted: 21 August 2011 / Published online: 24 September 2011
© ISS 2011

Abstract
Objective The objective of this work was to evaluate the potential of diagnostic imaging in the identification, localization, and characterization of soft-tissue inflammatory myofibroblastic tumors (IMTs) of limbs with correlation to differential diagnosis and therapy.
Materials and methods From a retrospective analysis of 324 histologically verified soft-tissue lesions of limbs and extremities diagnosed in our institute from January 2002 to July 2010, we selected seven cases of histologically proven IMT. These included six males and one female, aged between 28 and 81 years (mean age, 57 years). Lesions were localized in three cases to the thigh, in two cases to the popliteal space, and in the remaining two cases, to the shoulder girdle. All patients were evaluated on the basis of US, CT, and MRI.
Results Ultrasound detected the presence of a non-homogeneous solid formation in all cases and calcifications in three cases. CT showed the presence and type of calcification/ossification and bone reaction. On MRI, all cases had low signal intensity on SE T1-weighted sequences and an intermediate–low signal intensity on SE and FSE T2-weighted sequences in six of them; only one case had an intermediate–high signal intensity on SE and FSE T2-weighted sequences. Both contrast-enhanced CT and MRI showed precocious enhancement in association with multiple peripheral hypertrophic blood vessels.
Conclusions On the basis of integrated imaging data obtained by US, CT, and MRI, it is possible to evaluate the lesion extension to provide a loco-regional staging, to characterize IMTs, and to allow an optimal therapeutical planning.

Keywords Soft-tissue tumors · Inflammatory myofibroblastic tumors · Diagnostic imaging modalities · Ultrasound · Computed tomography · Magnetic resonance imaging

C. Masciocchi · G. Lanni · L. Conti · A. Conchiglia · E. Fascetti · A. Barile (✉)
Department of Radiology,
University of L'Aquila, S. Salvatore Hospital,
Coppito 67100 L'Aquila, Italy
e-mail: abarile63@me.com

S. Flamini
Department of Orthopaedic Surgery,
S. Salvatore Hospital,
Coppito, L'Aquila, Italy

G. Coletti
Department of Pathology,
S. Salvatore Hospital,
Coppito, L'Aquila, Italy

Introduction

Inflammatory myofibroblastic tumors (IMTs) or inflammatory pseudotumors include a heterogeneous group of lesions, first described in 1954 by Umiker [1], histologically characterized by a dominant spindle cell proliferation with a variable inflammatory and fibrotic component [2–8], and have been defined as inflammatory lesions [8–10].

The histological origin of IMTs is controversial and both diagnostic approaches and therapeutic strategies remain the subject of debate. As reported in the literature, IMTs most commonly occur in the lung and retroperitoneum [11–13]. However, other locations are observed causing serious diagnostic difficulties and, due to their locally aggressive nature, make for difficult therapeutic choices [14–17].

Little attention has been paid to IMTs' localization in limbs and extremities [18, 19]. At these sites, the identification of an expansive lesion combined with locally

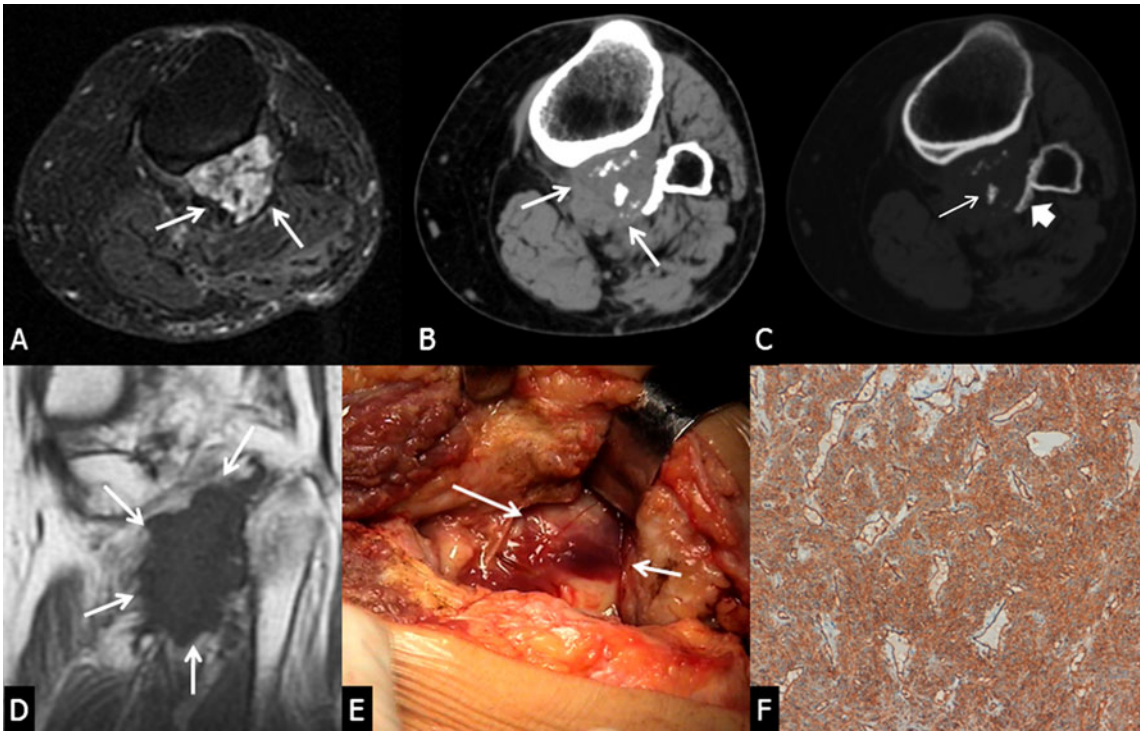

Fig. 1 IMT of left leg. MR axial FSE T2-weighted fat-saturated image (**a**) shows the presence of inhomogeneous polylobulated mass at the level of popliteal fossa (*arrows*). CT scan (**b**) confirms the presence of inhomogeneous mass (*arrows*) and the same CT slice with bone window (**c**) better defines the presence of central-lesional areas of non-structured and non-confluent gross calcifications (*thin arrow*) and "shell-like" periosteal reaction (*large arrow*). **d** Coronal SE T1-weighted image depicts longitudinal extension of the lesion (*arrows*). **e** Intraoperative view of the lesion (*arrows*). **f** Histology (immunohistochemical staining using antibodies against actin) confirms the myofibroblastic origin of the lesion

aggressive features creates problems in differential diagnosis with malignant neoplasms, which not only require demolitive surgical approaches but also post-surgical chemo and radiotherapy. In these cases, correct diagnosis is particularly useful in planning therapy.

Although IMTs of long bone have recently been described [19], to our knowledge, no radiological data regarding soft-tissue IMTs of limbs have been reported. Therefore, the aim of this retrospective study was to evaluate the potential of diagnostic imaging in the identification, localization, and characterization of soft-tissue IMTs of limbs with correlation to differential diagnosis and therapy.

Materials and methods

From a retrospective analysis of 324 soft-tissue lesions of limbs and extremities diagnosed in our institute from January 2002 to July 2010, we selected seven cases of histopathologically proven IMT. These included six male and one female patient aged between 28 and 81 years (mean age, 57 years). Lesions were localized in three cases to the thigh, in two cases to the popliteal space, and in the remaining two cases, to the shoulder girdle. No history of former pathologies was found in six of them. The oldest patient had undergone surgical treatment 3 years prior to diagnosis for a lipoma-like liposarcoma of the left thigh and subsequently developed an expansive lesion in the same region. All patients had previously undergone ultrasound examination on the basis of clinical suspicion of soft-tissue mass.

CT examination, performed with a three-dimensional six-row multidetector CT scanning (Brilliance 6, Philips Medical Systems, Eindhoven, The Netherlands), was done in all cases with and without contrast agent (Iobitridol 350). MR examination was performed with and without contrast agent (Gd-DOTA) in all patients; in five patients contrast-enhanced MR examination was performed using a dynamic technique.

MRI was performed on axial, coronal, and sagittal scan planes, using a 1.5-Tesla unit (GE Signa Horizon, Milwaukee, WI, USA). The imaging protocol for all examinations included STIR sequence (TR/TE, 3500-6000/55 ms; inversion time, 150 ms), spin-echo (SE) T1-weighted with and without fat-suppression sequence (TR/TE, 300-420/9-16 ms), spin-echo (SE) and fast spin-echo (FSE) T2-weighted with and without fat-suppression sequence (3,500-5000/57-100 ms).

All patients were biopsied (a 16–18 G Tru-cut needle were used), using US guidance in six and CT with multi-sample

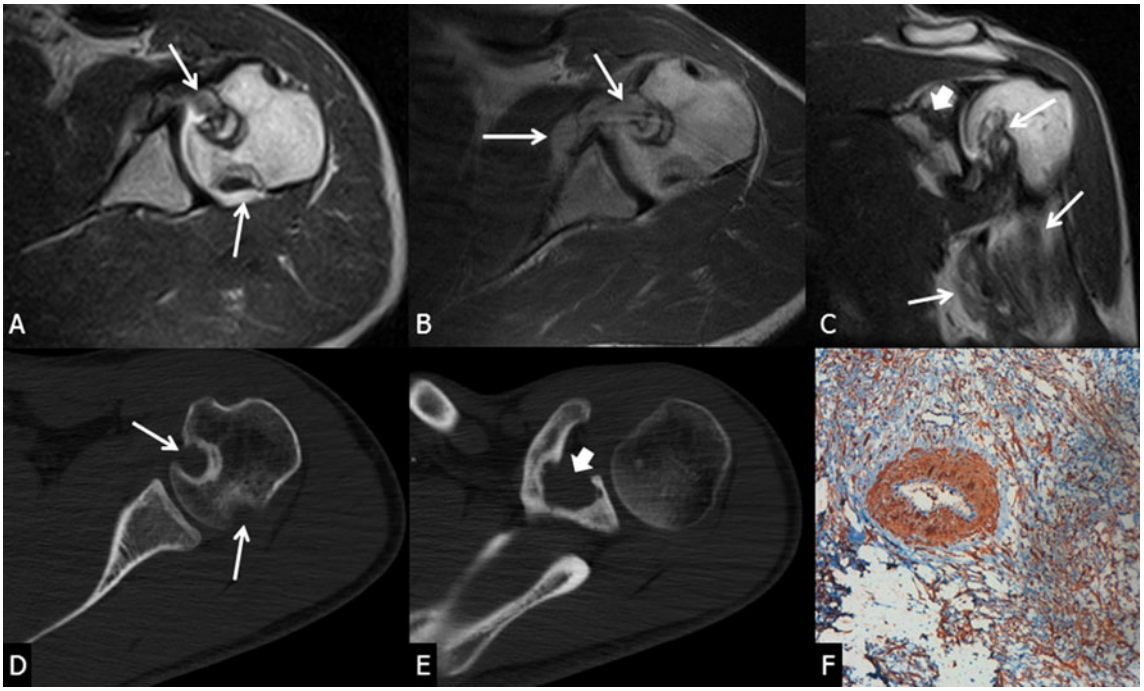

Fig. 2 IMT of shoulder girdle. MR axial FSE T2-weighted image (**a**) shows osseous humeral head lesion (*arrows*); MR axial SE T1-weighted image (**b**) after administration of contrast agent shows the presence of enhanced tissue at the level of the anterior portion of the joint (*arrows*). Coronal SE T2-weighted image (**c**) well documented the presence of intermediate–low signal intensity tissue at the level of upper arm (*arrows*) with involvement of humeral head; glenoid bone is also involved (*large white arrow*). CT scans (**d**, **e**) better depict focal osteolytic lesion of the humeral head (*long white arrows* in **d**) and of the glenoid (*large white arrow* in **e**). Histology (**f**) (immunohistochemical staining using antibodies against actin) confirms the presence of actin-positive cells

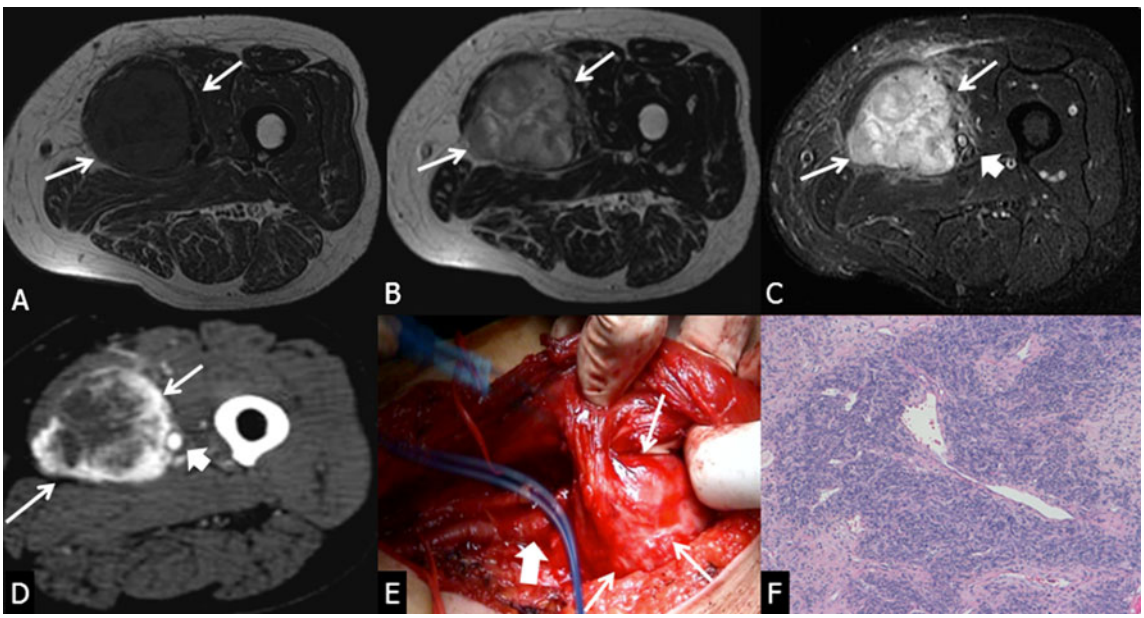

Fig. 3 IMT of the thigh. **a** MR axial SE T1-weighted image shows space-occupying lesion (*arrows*) at the level of antero-medial compartment of thigh with close relationship with blood vessels. MR axial FSE T2-weighted images without (**b**) and with (**c**) fat suppression on the same plane show the intermediate-low signal intensity of the mass (*long arrows*); note compressed and displaced blood vessels (*large arrow* in **c**). **d** CT-angiography image at similar level shows intense and precocious enhancement of the lesion (*arrows*) and confirms the close relationship with femoral artery, as confirmed at surgery (**e**) (*large arrows*). Histology (**f**) (hematoxylin and eosin staining) confirms inflammatory origin of the lesion

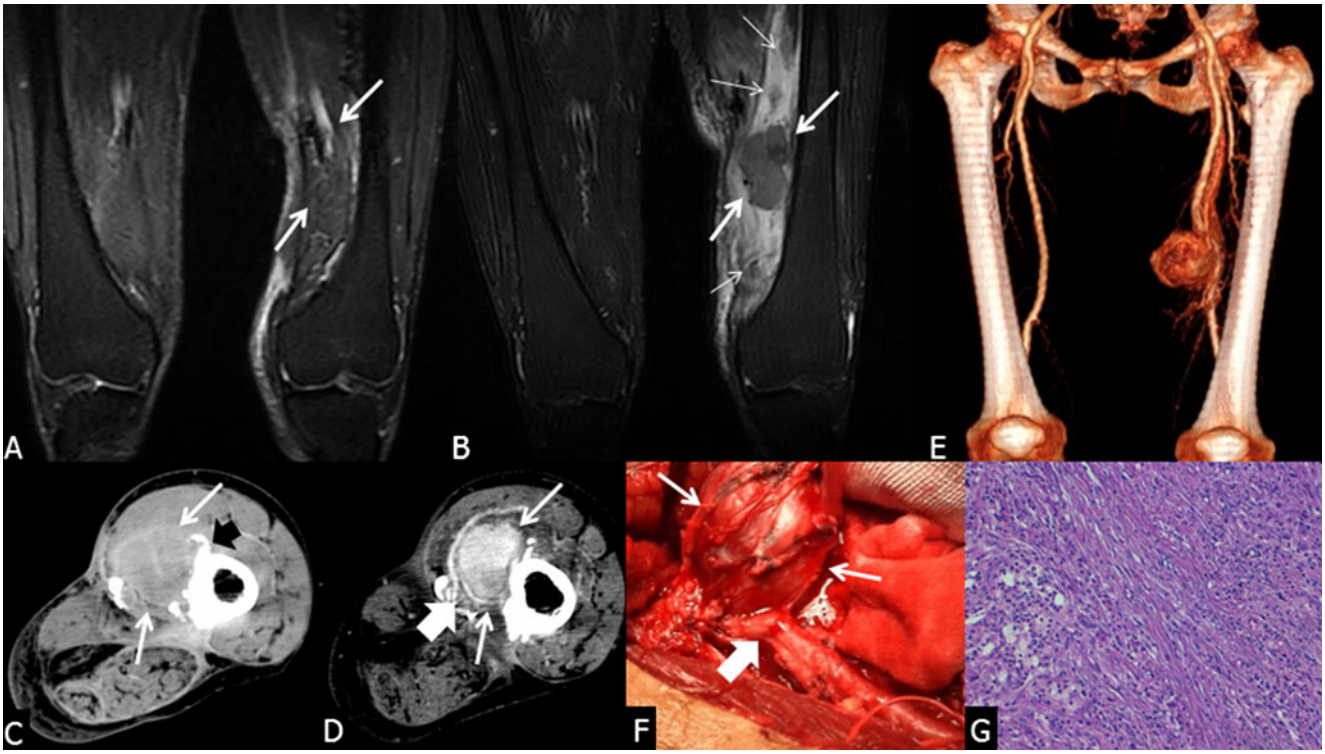

Fig. 4 IMT of left thigh in a patient previously treated for lipoma-like liposarcoma. **a** MR coronal FSE T2-weighted fat-saturated image performed after surgical treatment of lipoma-like liposarcoma shows the absence of space-occupying lesion (*arrows*) (see the asymmetric muscle volume of the thighs. **b** MR coronal FSE T2-weighted fat-saturated image performed 3 years later shows a polylobulated low-signal intensity mass of antero-medial compartment of thigh (*arrows*); note the presence of wide extent of associated edema of the medial compartment of the tight (*thin arrows*). **c** CT scan shows the mass (*white arrows*) and the presence of "shell-like" periosteal reaction (*black arrow*). **d** CT-angiography image at similar level shows intense and precocious enhancement of the lesion with the presence of peripheral hypertrophic vessels (*long white arrows*); the adherence of the mass with femoral artery is also seen (*large white arrow*). CT-angiography 3D reconstruction (**e**) and surgery (**f**) confirm the adherence of the mass (*long white arrows*) with the femoral vessels (*large white arrow*). Histology (**g**) (hematoxylin and eosin staining) confirms the inflammatory origin of the lesion

technique in one patient (a minimum of four different biopsies were taken from different areas of the lesion).

Six patients were treated surgically; five underwent lesion excision and one limb amputation. This patient exhibited disease localization to the shoulder girdle with gleno-humeral joint involvement, making amputation of the superior limb an unavoidable necessity.

The remaining one patient with IMT localized to the popliteal space did not undergo surgery after biopsy due to close lesion relationship to vascular structures and absence of symptomatology. This patient was followed-up by MR every 6 months, which indicated relative lesion stability in the absence of progression (to date, the patient has been followed-up for 4 years).

Results

In all cases, the histopathological diagnosis, including immunohistochemical study using antibodies against actin, was IMT. Ultrasound, performed in all patients without administration of contrast agent, detected the presence of a non-homogeneous solid formation; in six patients the mass had well-defined borders while in the patient with a localization at the level of the shoulder girdle, the mass appeared irregular and with badly defined borders.

Ultrasound detected both intralesional and peripheral, lamellar-shaped calcifications in one patient and in two patients only peripheral, lamellar-shaped calcifications were detected.

CT examinations were performed in all cases with and without intravenous administration of contrast agent. The lesions always exhibited precocious enhancement in association with multiple peripheral hypertrophic blood vessels. In one patient, CT scans detected gross non-structured, non-confluent calcifications at the lesion center with "shell-like" periosteal reaction and partial cortical scalloping (Fig. 1).

In the other two patients, "shell-like" periosteal reactions that partially surrounded the lesion were observed. In the other one patient, only a partial cortical scalloping without erosion was demonstrated.

In one patient with the lesion localized to the shoulder girdle with gleno-humeral joint extension, the mass

Table 1 Diagnostic imaging, surgery, and histological patterns of IMTs

Patient	Localization	US			CT				MRI			Surgery	Histology
		Echoic pattern	Borders	Calcifications	Type of calcification/ossification		Bone reaction		CE	Signal intensity		CE	
					Central, non-structured/ non-confluent	"Shell-like" periosteal	Cortical scalloping	Erosion		T1W	T2W		
1	Left leg	Hypo/Inho	Def	C/P	Y	Y	Y	N	Y	L	I-H	Y	Exc	IMT
2	Left thigh	Hypo/Inho	Def	P	N	Y	N	N	Y	L	I-L	Y	Exc	IMT
3	Right leg	Hypo/Inho	Def	P	N	Y	Y	N	Y	L	I-L	Y	N - FU	IMT
4	Shoulder girdle	Hypo/Inho	Def	N	N	N	N	N	Y	L	I-L	Y	Exc	IMT
5	Left thigh	Hypo/Inho	Def	N	N	N	N	N	Y	L	I-L	Y	Exc	IMT
6	Right thigh	Hypo/Inho	Def	N	N	N	N	N	Y	L	I-L	Y	Exc	IMT
7	Shoulder girdle	Hypo/Inho	N-Def	N	N	N	N	Y	Y	L	I-L	Y	Amp	IMT

Hypo hypoechoic; *Inho* inhomogeneous; *Def* definite; *N-Def* non-definite; *C* central; *P* peripheral; *Y* yes; *N* no; *L* low; *I* Intermediate; *H* high; *Amp* surgical amputation; *Exc* surgical excision; *FU* follow-up; *CE* contrast enhancement

exhibited glenoid infiltration with pseudo-erosive phenomena of both the superior and posterior humeral head also detected (Fig. 2).

MR was performed on all patients with and without intravenous administration of paramagnetic contrast agent using a standardized dynamic technique for vascular evaluation of neoplastic lesions. On plain scans, six lesions exhibited a low signal intensity on SE T1-weighted sequences and an intermediate-low signal intensity on T2-weighted sequences, both SE and FSE with central inhomogeneity (Fig. 3). In one patient with disease localized to the popliteal space, a homogeneous "cluster-like" form was detected, associated with low signal intensity on SE T1-weighted sequences and intermediate–high signal intensity on T2-weighted sequences.

After intravenous administration of paramagnetic contrast agent, all patients showed intense enhancement of arterial phase followed by a rapid wash-out with peripheral accumulation of contrast agent. In four patients, peripheral hypertrophic blood vessels were detected. Calcifications and periosteal reactions could not be clearly assessed by MR. Surgery was performed in six cases. In one patient, lesion borders could not be detected using US, CT, or MR due to localization within the shoulder girdle combined, with gleno-humeral joint extension, muscular structure displacement and presence of the articular capsule.

For this reason, radical surgical amputation of the superior limb was necessary to obtain a therapeutic result. In the other five patients, surgery confirmed US, CT, and MR data regarding both the site and extension of the lesion its relationship to adjacent muscular, fascial, adipose, and vascular structures (Fig. 4).

Our results are summarized in Table 1.

Discussion

Inflammatory pseudotumors are infrequent lesions with an unclear etiological, clinical, and diagnostic classification. Although their etiology is unknown, an inflammatory origin has been suggested due to an association with minor trauma, surgery, and/or infections. Although histologically lesions are predominated by myofibroblasts, many different classes, exhibiting differences in cellular content and histology, are included within this large group. Today, these lesions are grouped under the term of IMT, as defined by the WHO. The chest represents the most common localization for IMTs with rare limb and extremity involvement. Within the limbs, IMT lesions are not easily distinguished from more aggressive malignant tumors, which require radical surgical removal and subsequent aggressive chemo and radiotherapy. Diagnostic imaging, therefore, plays a fundamental role not only in lesion

identification but also in preliminary lesion characterization [20–23].

Although final diagnosis depends upon biopsy, lesions cannot be easily assessed histologically without prior imaging. In fact, imaging is essential not only for mass detection but also (and above all) for the loco-regional staging of the lesion, defining margins, relationship to surrounding structures, displacement of muscular mass, footprint, and relationship to skeletal and neurovascular structures. The combination of different imaging techniques, therefore, plays a crucial role in defining the nature and biology of IMTs.

To our knowledge, in all cases of IMTs reported in the literature, the imaging of soft-tissue inflammatory pseudotumors in extremities and limbs has not been described. Here, we directly address this issue by describing imaging parameters for use in the characterization of IMTs prior to biopsy.

Calcifications, in our experience, were present within the mass in one patient. These exhibited a dystrophic appearance due to the precipitation of calcium salts during inflammation, edema, and vascular anomalies. In three patients, we found thin calcifications of pseudo-lamellar appearance, in addition to the presence of a pseudo-capsule this information is crucial for the characterization of IMTs, as poorly infiltrative less aggressive lesions, with inflammatory phenomena promoting new bone production may mimic IMT.

Another important element when characterizing lesions is the detection of cortical bone adaptive phenomena, when the inflammatory mass is located on the parosteal side, which was observed in two patients.

In one patient, there was some erosion of the scapular glenoid and the humeral head, with a pseudo-infiltrative appearance, probably due to the high local aggressiveness of this lesion. In this case, amputation was necessary in order to achieve an adequate therapeutic outcome.

All patients underwent CT and MRI with and without contrast agent. Contrast enhancement was invariably observed in the vascular phase in both CT and MRI, although contrast impregnation was not homogeneous, from the periphery to the center of the lesion. In all cases, a rapid washout was observed leaving vast areas of non-homogeneous enhancement. A common feature of these forms was close location and relationship with major vascular structures, confirming that IMTs adhere to vessels and adventitia. In addition, in four patients, interactions with peripheral and hypertrophic vascular structures were clearly recognized by CT and MRI, and confirmed by subsequent surgical exploration and macroscopic evaluation. In three patients, hypertrophic vascularization caused significant bleeding during biopsy, which was easily controlled by appropriate compression. CT and MRI showed excellent accuracy in assessing lesion vascularity, in defining the components of peripheral hypertrophic vascularity, and the relationship of lesions to adjacent vascular structures. MRI also facilitated lesion characterization, as it detected intermediate to low signal intensity on T2-weighted sequences with non-homogeneous areas, particularly in the central region. This was probably due to the central presence of myofibroblastic cells, which also helps to explain histological features. Another important role for diagnostic imaging is to define the extension of the lesion required, following biopsy, to determine the surgical approach, which must be radical due to the tendency for local recurrence.

In summary, IMTs of the limbs are rare and may mimic malignant neoplasms. Although none of the diagnostic techniques on their own should be used in evaluating and defining IMT, the combined use of US, CT, and MR provides the best structural analysis of IMT lesion defining borders, localization, and relationship with adjacent structures. In our experience, the combination of CT and MR provides the greatest advantage in loco-regional staging and in detecting peculiar elements within lesions, such as type of calcification/ossification, adaptative phenomena of bone in patients with progressively worsening pain, which represents an important clinico-radiological element in the differential diagnosis of IMTs from malignant neoplasms.

References

1. Umiker WO, Iverson L. Postinflammatory tumors of the lung; report of four cases simulating xanthoma, fibroma, or plasma cell tumor. J Thorac Surg. 1954;28:55–63.
2. Cessna MH, Zhou H, Sanger WG, Perkins SL, Tripp S, Pickering D, et al. Expression of ALK1 and p80 in inflammatory myofibroblastic tumor and its mesenchymal mimics: a study of 135 cases. Mod Pathol. 2002;15(9):931–8.
3. Sigel JE, Smith TA, Reith JD, Goldblum JR. Immunohistochemical analysis of anaplastic lymphoma kinase expression in deep soft tissue calcifying fibrous pseudotumor: evidence of a late sclerosing stage of inflammatory myofibroblastic tumor? Ann Diagn Pathol. 2001;5(1):10–4.
4. Stoll LM, Li QK. Cytology of fine-needle aspiration of inflammatory myofibroblastic tumor. Diagn Cytopathol. 2010 Aug 20.
5. Coffin CM, Patel A, Perkins S, Elenitoba-Johnson KS, Perlman E, Griffin CA. ALK and p80 expression and chromosomal rearrangements involving 2p23 in inflammatory myofibroblastic tumor. Mod Pathol. 2001;14:569–76.
6. Wenig BM, Devaney K, Bisceglia M. Inflammatory myofibro- blastic tumor of the larynx. A clinicopathologic study of eight cases simulating a malignant spindle cell neoplasm. Cancer. 1995;76:2217–29.
7. Pettinato G, Manivel JC, De Rosa N, Dehner LP. Inflammatory myofibroblastic tumor (plasma cell granuloma): clinicopathologic study of 20 cases with immunohistochemical and ultrastructural observations. Am J Clin Pathol. 1990;94:538–46.
8. Cook JR, Dehner LP, Collins MH, et al. Anaplastic lymphoma kinase (ALK) expression in the inflammatory myofibroblastic tumor: a comparative immunohistochemical study. Am J Surg Pathol. 2001;25:1364–71.
9. Chan JKC. Inflammatory pseudotumor: a family of lesions of diverse nature and etiologies. Adv Anat Pathol. 1996;3:156–69.

10. Batsakis JG, El-Naggar AK, Luna MA, Geopfert H. Inflammatory pseudotumor: what is it? How does it behave? Ann Otol Rhinol Laryngol. 1995;104:329–31.
11. Meis JM, Enzinger FM. Inflammatory fibrosarcoma of the mesentery and retroperitoneum. A tumor closely simulating inflammatory pseudotumor. Am J Surg Pathol. 1991;15:1146–56.
12. Koirala R, Shakya VC, Agrawal CS, Khaniya S, Pandey SR, Adhikary S, et al. Retroperitoneal inflammatory myofibroblastic tumor. Am J Surg. 2010;199(2):e17–9.
13. Sleigh KA, Lai W, Keen CE, Berrisford RG. Calcifying fibrous pseudotumours: an unusual case with multiple pleural and mediastinal lesions. Interact Cardiovasc Thorac Surg. 2010;10 (4):652–3.
14. Schütte K, Kandulski A, Kuester D, Meyer F, Wieners G, Schulz HU, et al. Inflammatory myofibroblastic tumor of the pancreatic head: an unusual cause of recurrent acute pancreatitis - Case presentation of a palliative approach after failed resection and review of the literature. Case Rep Gastroenterol. 2010;4(3):443–51.
15. Tunuguntla H, Mishra A, Jorda M, Gosalbez R. Inflammatory myofibroblastic tumor of the epididymis: case report and review of the literature. Urology. 2011;78(1):183–5.
16. Mariño-Enríquez A, Wang WL, Roy A, Lopez-Terrada D, Lazar AJ, Fletcher CD, et al. Epithelioid inflammatory myofibroblastic sarcoma: an aggressive intra-abdominal variant of inflammatory myofibroblastic tumor with nuclear membrane or perinuclear ALK. Am J Surg Pathol. 2011;35(1):135–44.
17. Son SB, Heo YS, Shin WW, Oh TS, Song HJ, Oh CH. A case of cutaneous inflammatory myofibroblastic tumor. Ann Dermatol. 2010;22(1):91–5.
18. Kransdorf MJ, Moser Jr RP, Meis JM, Meyer CA. Fat-containing soft-tissue masses of the extremities. Radiographics. 1991;11 (1):81–106.
19. Chen J, Li H, Yang Z, Liu Q, Gao M, Jiang X, et al. Inflammatory myofibroblastic tumor of bone: two cases occurring in long bone. Skeletal Radiol. 2011;40(1):117–22.
20. Navarro OM, Laffan EE, Ngan BY. Pediatric soft-tissue tumors and pseudotumors: MR imaging with pathologic correlation. Part 1. Imaging approach, pseudotumors, vascular lesions, and adipocytic tumors. Radiographics. 2009;29(3):887–906.
21. Siegel MJ. Magnetic resonance imaging of musculoskeletal soft tissue masses. Radiol Clin North Am. 2001;39:701–20.
22. Moulton JS, Blebea JS, Dunco DM, Braley SE, Bis-set 3rd GS, Emery KH. MR imaging of soft-tissue masses: diagnostic efficacy and value of distinguishing between benign and malignant lesions. AJR Am J Roentgenol. 1995;164:1191–9.
23. Ma LD. Magnetic resonance imaging of musculo-skeletal tumors: skeletal and soft tissue masses. Curr Probl Diagn Radiol. 1999;28:29–62.